
Article:
Cao, B., Zhao, J., Yang, P. orcid.org/0000-0002-8553-7127 et al. (4 more authors) (2020) Multi-objective 3D topology optimization of next generation wireless data center network. IEEE Transactions on Industrial Informatics, 16 (5). pp. 3597-3605. ISSN 1551-3203

https://doi.org/10.1109/TII.2019.2952565

Multi-Objective 3D Topology Optimization of Next Generation Wireless Data Center Network

***Abstract*—As one of the next generation network technologies for data centers, wireless data center network has important research significance. Smart architecture optimization and management are very important for wireless data center network. With the ever-increasing demand of data center resources, there are more and more data servers deployed. However, traditional wired links among servers are expensive and inflexible. Benefited from the development of intelligent optimization and other techniques, high-speed wireless topology for wireless data center network is studied. Through image processing, a radio propagation model is constructed based on a heat map. The line-of-sight issue and the interference problem are also discussed. By simultaneously considering objectives of coverage, propagation intensity and interference intensity as well as the constraint of connectivity, we formulate the topology optimization problem as a multi-objective optimization problem. To seek for solutions, we employ several state-of-the-art serial MOEAs as well as three parallel MOEAs. For the grouping in distributed parallel algorithms, prior knowledge is referred. Finally, experimental results demonstrate that, the parallel MOEAs perform effectively in optimization results and efficiently in time consumption.**

***Index Terms*—Multi-objective, topology optimization, wireless data center network, parallelism.**

I. Introduction

Wireless data center network (WDCN) is seen to be the next generation network technology for data center [1]–[3]. Smart architecture optimization and efficient management are important issues in WDCN [4]–[6]. Compared with wired communication technology, wireless communication technology has more advantages and better characteristics. First of all, wireless communication can not be restricted by wires, which greatly reduces the space occupancy. Secondly, the transmission characteristic of wireless communication through electromagnetic waves makes it more convenient than wired communication. At present, the wider and wider frequency band has been opened by all countries in the world, and intelligent optimization and other techniques are being pushed to the new height.

Data center is a complex facility that can accommodate multiple servers and communication devices. Its main role is to manage data in business and operation organizations by running applications. The network topology constructed by the various devices in the data center is called the data center network (DCN). With the progress of technology and the increasing demand of human beings, the drawbacks of wired DCN are more and more evident. The cable structure itself depends on the deployment of wires, and the increase of data center equipment will greatly increase the difficulty and cost of deployment. Besides, the difficulty of data center maintenance and reconfiguration will be very difficult. Therefore, the construction of wireless data center (WDC) is put on the agenda.

In recent years, all countries in the world have opened the license free bandwidth of more than 5GHz in the neighborhood of the 60GHz frequency. This makes the research of 60GHz wireless communication technology a new hotspot in the field of wireless communication. In 2008, Ramachandran et al. [7] first mentioned the application of 60GHz technology to WDCNs and proposed a hybrid wireless architecture as a wired communication extension [7].

60GHz wireless communication technology as a new technology, its advantages include not only anti-interference, security, high bandwidth and transmission rate, but also international universality and license-free characteristics, possessing high civil and commercial values. The application of 60GHz wireless communication technology is also very extensive. It can be used not only in smart home, automobile radar, medical imaging and other fields, but also in wireless high-definition multimedia equipment and inter-satellite communication because of its high transmission efficiency [8], [9]. Nevertheless, it has serious transmission loss in the air, and the particle characteristics of signal transmission are obvious, not ideal with respect to the indoor and outdoor transmission [10].

Through the use of 60GHz wireless communication technology, the construction of WDC has become possible. The problem is how to construct the topology of 60GHz radio more effectively, making wireless communication more efficient and less link-blocking.

Therefore, two wireless network topologies, Flyways [11] and 3D beamforming [12], were introduced in the literature. Flyways structure was easily blocked by obstacles. The 3D beamforming structure relied on higher ceilings, which should be flat without obstacles. Then a new type of Graphite structure [13] was introduced by manipulating the heights of wireless devices. The excellent performance of Graphite structure was proved by comparison on average nodal degree, coverage ratio, bisection bandwidth and average hop count.

The design of data center completely based on 60GHz radio frequency (RF) technology has been introduced in [14], which placed server nodes on the rack and built an irregular network topology model. Experiments showed that compared with wired data centers, WDCs based on 60GHz RF technology performed better in fault tolerance, delay and power consumption. The work of [15] studied and analyzed the scalability of WDC throughput using wireless multi-hop networks. Finally, a new speculative 2-partitioning scheme was proposed, which made wireless networks have higher throughput.

In the topology programming of WDCNs, targets under concern [13] include: link number, coverage ratio, bisection band-

width, average hop count, etc. To the best of our knowledge, only deterministic strategies are utilized to design the wireless topology [13], in which many assumptions are predefined and simplifications are conducted to facilitate analysis, thus, the final output will not be the optimal. Due to the characteristic of multiple targets, multi-objective evolutionary algorithms (MOEAs) [16], [17] can be utilized for optimization. For MOEAs, no prior knowledge is in need, while only the function values of all objectives are required. During the evolution of an MOEA, multiple objectives are simultaneously optimized, resulting in a set of solutions with different stress on different objectives. Mathematically, for a solution $\boldsymbol{x}$, we have:

$$F(\boldsymbol{x}) = (f_1(\boldsymbol{x}), f_2(\boldsymbol{x}), \ldots, f_M(\boldsymbol{x})) \tag{1}$$

where $F(\boldsymbol{x})$ denotes a point in the objective space, M is the number of objectives, and $f_i, i = 1, 2, \ldots, M$ represents the function value of objective i. For two points, $\boldsymbol{u}$ and $\boldsymbol{v}$, in the objective space, $\boldsymbol{u}$ is better than $\boldsymbol{v}$, if and only if $\boldsymbol{u}$ is not worse than $\boldsymbol{v}$ for all objectives and is better in at least one objective. Otherwise, they are nondominated to each other. And the final solution set will contain a number of nondominated solutions.

The contributions of this paper can be summarized as follows:

1) Based on the heat map in [13], through image processing and function fitting, a radio propagation model is constructed. For a given point inside the model, the propagation intensity can be obtained.
2) On the basis of the proposed propagation model, to tackle the signal blocking problem, the line-of-sight concept is introduced. Moreover, the interference calculation processing along the main signal is detailed.
3) We formulate the topology problem as a multi-objective problem (MOP) by simultaneously considering objectives of coverage, propagation intensity and interference intensity as well as the constraint of connectivity. To address the multi-objective topology optimization problem, several state-of-the-art serial MOEAs as well as distributed parallel MOEAs with prior knowledge-based grouping are employed.

For the remainder of this paper, the organization is as follows. The related works are discussed in Section II. Sections III and IV introduce the process of constructing the radio propagation model as well as the line-of-sight and interference discussion, respectively. In Section V, we detail the formulation of objectives in the considered topology optimization problem. The utilized algorithms are provided in Section VI. Followed in Section VII is the experimental analysis. Finally, we conclude this paper in Section VIII.

II. Related Works

Flyways [11] was proposed to enhance the congested wired DCN by implementing wireless devices on the top of racks. When the demand is moderate, the DCN can absolutely rely on the wired topology. In the case of over-subscription, the additional wireless links can provide extra bandwidth and improve quality of service. For the map-reduce workload, the hotspots are located at few switches, thus, flyways could deploy relatively few wireless devices to significantly improving DCN performance. However, flyways may not generalize to other service paradigms.

Wireless propagation is prone to blockage of obstacles along the propagation signal. In DCNs, traditionally, the racks are arranged regularly, and when deployed, the neighborhood of a wireless device will be restricted to those in adjacent racks. To alleviate blockage, Zhou et al. [12] introduced 3D beamforming via reflecting signals utilizing the ceiling. With respect to flat metal, concrete and plaster ceilings, the signal loss of reflection is little, while the signal can refrain from obstacles and the neighborhood can be extended. Conspicuously, the ceiling should be guaranteed flat and the signal length will increase via reflection.

From another aspect, Graphite structure [13] was introduced. The Graphite structure solved the problem of connection blockage by layering the radio and adjusting the height and angle of each radio. The topology of N layer Graphite has been expanded, but no excellent theoretical proof has been given. Specifically, in the two- or three-layer Graphite structure, the height constraints for communication between two different layers are given and the mathematical derivation is provided. Finally, the experimental results demonstrated the excellent performance of Graphite structure.

III. Radio Propagation Simulation

A. Radio to Matrix

Due to the different hardware designs of radio systems, the propagation of electromagnetic waves is not identical in different environments, therefore, the channel research must depend on practical situation. In [13], the radio propagation pattern was illustrated, with gray scale as in Fig. 1a, abstracted as a $\alpha = 9$-degree cone with the height of about $d_{Prop}^{th} = 10m$. When the distance is within d_{Prop}^{th}, it is regarded that the signal can be perceived. In this paper, we will establish a mathematical model of radio signals and give the probability distribution function for any position within d_{Prop}^{th}.

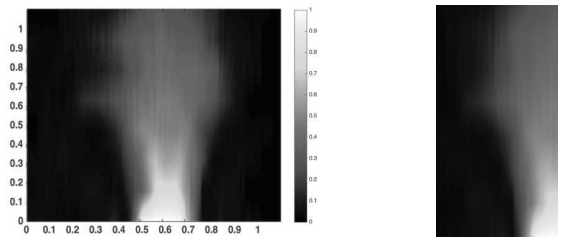

(a) Gray-scale pattern (b) Matrix

Fig. 1: Radio propagation illustration.

Transforming the picture into the gray-scale can better express the information conveyed by the picture. Through cropping and folding vertically to the main propagation direction, we simplify Fig. 1a to Fig. 1b, represented as a 2D matrix

[18] with each pixel in the range of $[0, 255]$. The higher the brightness of each pixel, the greater the propagation intensity.

B. Model Construction

According to the propagation matrix M_{prop}, for a target point, we can obtain the propagation intensity with respect to the transmitter (*i.e.*, the point, (x_c, y_c), in the lower right corner), as follows:

$$p_{prop}(d_f, d_v) = M_{prop}(x, y) \quad (2)$$
$$\text{s.t.} \begin{cases} x = \lceil x_c - d_f * n_x \rceil \\ y = \lceil y_c - d_v * n_y \rceil \end{cases}$$

where $p_{prop}(d_f, d_v)$ denotes the propagation intensity of the point with forward distance of d_f and vertical distance of d_v relative to (x_c, y_c), and n_x and n_y denote the numbers of units corresponding to one meter with respect to the x and y axes, respectively.

However, when d_v is too great to beyond the width of M_{prop}, $p_{prop}(d_f, d_v)$ is set as 0; on the contrary, when d_f is out of reach, we cannot simply set it to zero. To this end, we conduct distribution fitting to construct a model for prediction. Specifically, the samples are the upper portion of M_{prop} with $d_f \geq 8m$, and via the *Curve Fitting Tool* in MatLab, we can obtain the following model:

$$p_{prop}(d_f, d_v) = e^{-(\omega_1 d_v)^2 - \omega_2 d_f} \quad (3)$$

where $\omega_1 = 0.3628$ and $\omega_2 = 0.09763$ are parameters. And the fitting performance is illustrated in Fig. 2.

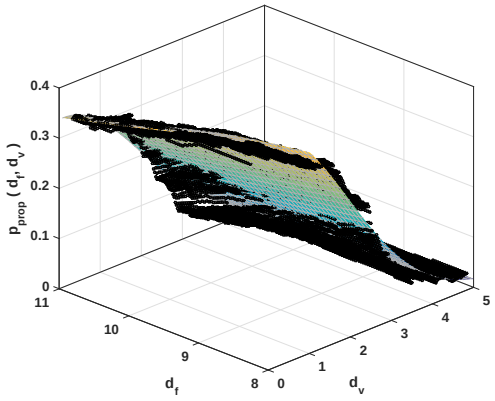

Fig. 2: Fitting performance.

IV. Line-of-sight (LOS) and Interference Discussion

A. LOS

Owing to its rotating characteristic, the wireless device is regarded as a sphere with the radius of $a = 0.1m$ [13], which can act as obstacles along the propagation path of the wireless signal. For this purpose, the LOS concept [19] is introduced. Specifically, a line is constructed connecting the two devices, the shortest distance of any other device should be larger than a.

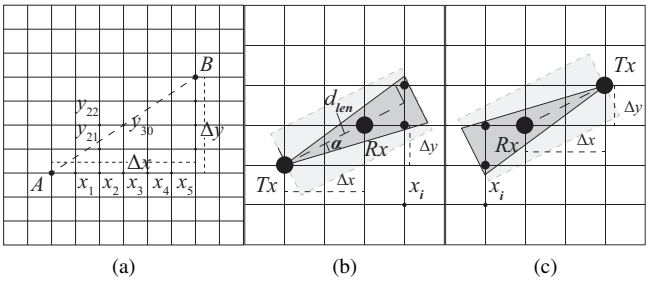

Fig. 3: LOS and interference processing.

For example, as illustrated in Fig. 3a, for two devices at points A and B, respectively, we first obtain the line AB. On the basis of the coordinates of A and B, we can calculate the position difference with respect to the horizontal and vertical coordinates: Δx and Δy. As $\Delta x > \Delta y$, we check the points along the x coordinate. Between the x coordinates of A and B, there are five x coordinates, corresponding to $x_1, x_2, \ldots, x_5$. For each x coordinate, the corresponding y coordinate at the line AB may not be an integer, such as x_2. In this case, as a is much smaller than the adjacent distance between racks, we only check y_{21} and y_{22}, while other values are ignored. For x_3, y_{30} is an integer, thus, no other y coordinates are checked.

B. Interference

Assuming one is the transmitter and the other the receiver, the propagation model can be constructed. There should not exist any other device, or the propagation probability at the position where any device locates should below P_{th}^{Prop}.

Take Fig. 3b and Fig. 3c for an instance, the checking zone is illustrated as a triangle (*i.e.*, the 2-D slice of a cone [13]). In Fig. 3b, we treat one as the transmitter Tx and the other the receiver Rx, and the checked points are marked by small black points; then, by changing their roles, we get Fig. 3c, and the same process will be done. In the above analysis, assuming $\Delta x > \Delta y$, for a checking coordinate x_i, the current signal length and checking width, d_{len} and d_{wid}, are computed, respectively, as follows:

$$d_{len}(i) = \text{abs}(x_i - x_{Tx}) \sqrt{1 + k^2} \quad (4)$$
$$d_{wid}(i) = d_{len}(i) \tan \alpha \quad (5)$$

where x_{Tx} denotes the x coordinate value of the transmitter Tx, then, the lower and higher checking lengthes along the y axis, l_{check}^{low} and l_{check}^{high}, respectively, will be:

$$\begin{aligned} l_{check}^{low}(i) &= \frac{d_{wid}(i)}{\sqrt{1+k^2}} - (y_i - \lfloor y_i \rfloor) \\ &= \text{abs}(x_i - x_{Tx}) \tan \alpha - (y_i - \lfloor y_i \rfloor) \end{aligned} \quad (6)$$

$$\begin{aligned} l_{check}^{high}(i) &= \frac{d_{wid}(i)}{\sqrt{1+k^2}} + (y_i - \lfloor y_i \rfloor) \\ &= \text{abs}(x_i - x_{Tx}) \tan \alpha + (y_i - \lfloor y_i \rfloor) \end{aligned} \quad (7)$$

where k is the slope of the line connecting Tx and Rx, and y_i denotes the currently checked y coordinate value.

Through the above interference analysis, the interference to devices in the checking cone is restricted to less than P_{th}^{Prop}. Additionally, we need to calculate the interference intensity

at devices in the cylinder around the signal, illustrated as a rectangle in Fig. 3b and Fig. 3c. The process is similar to the above, except that $d_{wid}(i) = d_{wid}^{max}$ as predefined.

V. Problem Formulation of Multi-Objective Topology Optimization

A. Individual Expression

For an MOEA, a population of individuals in the solution space are maintained, for each individual, which contains a set of variables, through the objective functions, the objective values are obtained, corresponding to a point in the objective space. During evolution, an MOEA aims to search the solution space to collect a set of points with better objective values.

In the WDCN, there are N_{radio} wireless devices, with the distance between two adjacent devices of D_{gap}. The deployment positions of devices are fixed on the top of racks. As in [13], the height and transmission direction of each device are flexible, however, in [13], several layers are formed and the heights of devices are fixed to one layer. This configuration exerts heavy constraint to the device height to facilitate the mathematical analysis, nevertheless, it may not lead to the ideal result. Therefore, we treat each height as a variable, and by optimizing them utilizing MOEAs, we are eager to explore whether better results can be obtained. Specifically, we have:

$$\begin{aligned} \boldsymbol{x}_i &= (x_{i,1}, x_{i,2}, \ldots, x_{i,N_{radio}}) \\ &\text{s.t. } i = 1, 2, \ldots, NP. \end{aligned} \tag{8}$$

where $\boldsymbol{x}_i$ denotes individual i, NP is the population size, and $x_{i,j}, j = 1, \ldots, N_{radio}$ represents the height of device j. Given the heights of all devices, we can calculate the function values of the objectives as in the following subsections.

B. Coverage

The coverage of a wireless device denotes its connection status with other ones within its communication range. The more the formed connections, the more the topologies can be designed, and the better the network will be. The formulation of this objective, f_{COV}, is as follows:

$$f_{COV} = 1.0 - \frac{1}{N_{radio}} \sum_{i=1}^{N_{radio}} \frac{N_i^L}{N_i^{L,max}} \tag{9}$$

where N_i^L denotes the formed link number of device i, and $N_i^{L,max}$ represents its maximum link number. By minimizing f_{COV}, a MOEA can maximize the mean average coverage degree, thus, the overall coverage of the network can be maximized.

C. Propagation Intensity

The propagation intensity of the radio signal denotes the communication quality from the transmitter to the receiver, and better intensity indicates higher transmission band width. For this objective, f_{PRI}, we have:

$$\overline{P_i^P} = \sum_{j \in S_i^N} \frac{P_{i,j}^P}{\left|S_i^N\right|} \tag{10}$$

$$f_{PRI} = 1.0 - \frac{1}{N_{radio}} \sum_{i=1}^{N_{radio}} \overline{P_i^P} \tag{11}$$

where $\overline{P_i^P}$ is the average propagation intensity of device i, S_i^N denotes the set of devices in the neighborhood of device i, in which, device i can communicate with them directly, $\left|S_i^N\right|$ is the cardinality of set S_i^N, and $P_{i,j}^P$ represents the propagation intensity of the radio signal between devices i and j.

D. Interference Intensity

In the former section, the mean average propagation intensity is to be maximized, however, if the interference is not under concern, some devices can be badly interfered and the overall network quality will reduce. By minimizing the interference intensity, this problem can be addressed to some extent. Therefore, formulate the interference intensity objective, f_{INT}, as follows:

$$f_{INT} = \frac{1}{N_{radio}} \sum_{i=1}^{N_{radio}} \frac{\sum_{1 \le j \le N_{radio}, k \in S_j^N} P_{j,k,i}^I}{2N_i^{L,max}} \tag{12}$$

where $P_{j,k,i}^I$ denotes the interference intensity in device i when transmitter device j communicates with receiver device k.

E. Connectivity Constraint

In the WDCN, any two wireless devices should be able to communicate to each other directly or indirectly by using other devices as hops. For this purpose, the connectivity constraint is exerted. Specifically, the WDCN forms an undirected graph. In which, a vertex represents a wireless device on the top of a rack, and a line between two vertices denote the connection status of the two devices, that is, if they can communicate with each other, there exists an edge, and vice versa. Based on the graph theory, we can find the maximal connected subgraph, and if its cardinality, N_{radio}^{MCSG}, is equivalent to N_{radio}, the connectivity constraint is fulfilled, otherwise, we have:

$$f_{penalty} = \left(N_{radio} - N_{radio}^{MCSG}\right) \times v_p \tag{13}$$

where $f_{penalty}$ denotes the penalty function value, and v_p represents the penalty value, which is arbitrarily large, here, we simply set it as 10^6.

F. Objective Discussion

For each MOEA, the optimization target will be

$$\min \begin{cases} f_{COV} + f_{penalty} \\ f_{PRI} + f_{penalty} \\ f_{INT} + f_{penalty} \end{cases} \tag{14}$$

Due to $f_{penalty}$, the MOEA first checks whether the connectivity constraint is satisfied or not. As to the objective value

ranges, from Eqs. 9, 11 and 12, we can know all three objective values are in the range of $[0, 1]$.

By optimizing f_{COV}, more links can be formed; f_{PRI} encourages the MOEA to produce solutions with better links; f_{INT} ensures that the propagation interference will not too much; simultaneously considering all three objectives, high-quality topologies with more better links can be formed.

VI. Algorithms Employed

A. Serial Algorithms

To tackle the multi-objective topology optimization problem, we employ several state-of-the-art MOEAs, including Cooperative Coevolutionary Generalized Differential Evolution 3 (CCGDE3) [20], Cooperative Multi-Objective Differential Evolution (CMODE) [21], Multiobjective Evolutionary Algorithm based on Decomposition (MOEA/D) [17], Multi-objective Evolutionary Algorithm based on Decision Variable Analyses (MOEA/DVA) [22], Nondominated Sorting Genetic Algorithm II (NSGA-II) [16], Nondominated Sorting Genetic Algorithm III (NSGA-III) [23]. We summarize their characteristics in Table I.

TABLE I: Serial Algorithm Summary

Algorithm	Principle	Large-Scale	Grouping
CMODE	Pareto nondominance	No	No
NSGA-II		No	No
CCGDE3		Yes	Yes
MOEA/D	decomposition	No	No
MOEA/DVA		Yes	Yes
NSGA-III	reference points	No	No

B. Distributed Parallel Algorithms

For the distributed MOEAs, we select the following: Distributed Parallel Cooperative Coevolutionary Multi-Objective Evolutionary Algorithm (DPCCMOEA) [24], Distributed Parallel Cooperative Coevolutionary Multi-Objective Evolutionary Algorithm (DPCCMOLSEA) [25]. and Distributed Parallel Cooperative Coevolutionary Multi-Objective Large-Scale Immune Algorithm (DPCCMOLSIA) [26]. The summary of all parallel algorithms is listed in Table II.

TABLE II: Parallel Algorithm Summary

Algorithm	Principle	Distributed model [27]	Objective Decomposition
DPCCMOEA	decomposition	island	No
DPCCMOLSEA		hierarchical	No
DPCCMOLSIA		hierarchical	Yes

C. Prior knowledge based Grouping

In the distributed algorithms, originally, the variable grouping is realizes through variable property analysis and dependency examination. While for a specific MOP, the utilization of prior knowledge can guarantee the grouping accuracy and reduce the waste of FEs. Therefore, variables are grouped in advance based on our understanding of the considered MOP. Specifically, as the WDCN forms a rectangle, devices are uniformly separated to four parts: the upper left, the upper right, the lower left and the lower right.

D. Summary

In the considered WDCN, the number of devices can be large [13], correspondingly, the MOP will be large in scale. Besides, the computation of the objective functions will be time-consuming. Compared to serial MOEAs, the distributed parallel algorithms will be more efficient in operation time. In addition, as the CC framework is employed in all distributed algorithms, their optimization performance can also be satisfying.

VII. Experimental Study

A. Parameter Settings

1) Model Parameters: Based on the work of [13], the propagation distance is set to $d^{th}_{Prop} = 10m$ and $15m$. The checking angle in Fig. 3 of subsection IV-B is set to $\alpha = 0.01\pi$. For interference calculation, we set $d^{max}_{wid} = 3m$. The racks form a matrix of 20×20 with the adjacent distance of $3m$. The distance from the top of the rack to the ceiling is $4m$.

TABLE III: Algorithm Parameter Settings

Symbol	Attribute	Quantity
	differential evolution (DE) [28]	
F	weighting factor	0.5
CR	crossover rate	1.0
	simulated binary crossover (SBX)	
p_c	crossover probability	1.0
η_c	distribution index	20
	polynomial mutation	
p_m	mutation probability	$1/nDim$
η_m	distribution index	20
	MOEA/D framework	
$niche$	neighborhood size	$0.1 \times NP$
$limit$	replace limit	2
P_{slct}	parent selection probability	0.9

2) Algorithm Parameters: For the two different d^{th}_{Prop} values, we run each algorithm 24 times, each with the number of fitness evaluations (FEs) set as $D \times 10^4$, and $D = N_{radio}$ is the number of variables. The population size is $NP = 120$. Specifically, CCGDE3 randomly segregates variables to 2 species, each contains 60 individuals. For CMODE, the swarm size is 20 and the archive size is $NP = 120$. For other detailed parameter settings, please refer to Table III. Additionally, for the distributed parallel algorithms, the number of CPUs employed is 72.

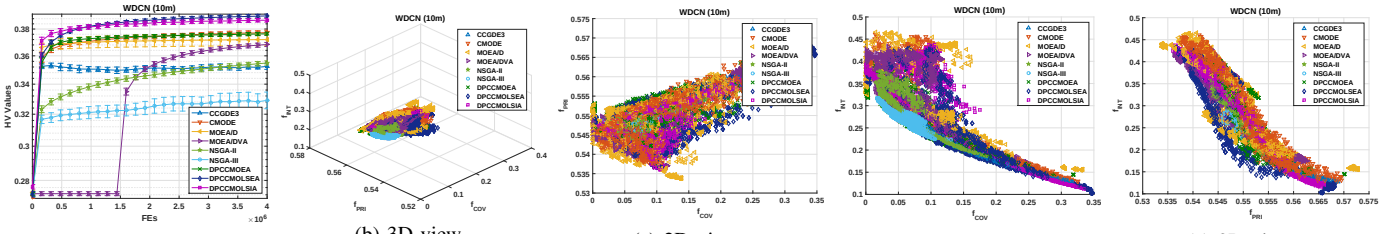

(a) HV (b) 3D view (c) 2D view (d) 2D view (e) 2D view

Fig. 4: HV indicator and solution visualization ($10m$).

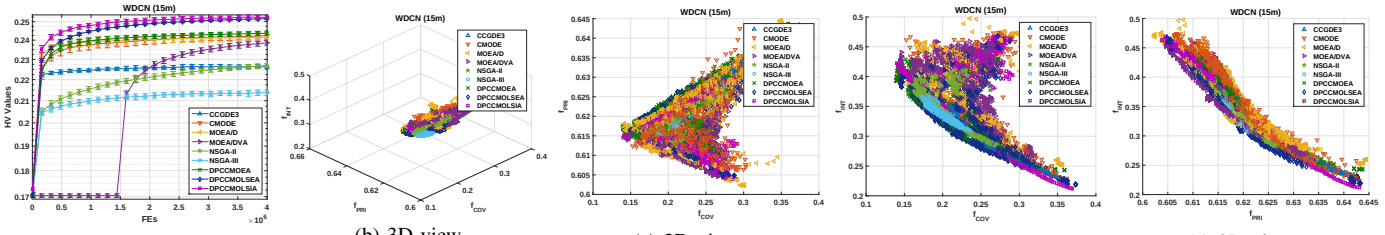

(a) HV (b) 3D view (c) 2D view (d) 2D view (e) 2D view

Fig. 5: HV indicator and solution visualization ($15m$).

B. Performance Indicator

There are various indicators [29] such as inverted generational distance (IGD), hypervolume (HV), etc. Nevertheless, IGD requires the Pareto optimal front, which is unknown for the multi-objective topology optimization problem, while HV can still evaluate the obtained Pareto front regardless of this prior knowledge, therefore, in this paper, the HV indicator is utilized, for which, we set the reference as $(1.0, 1.0, 1.0)$.

C. Optimization Performance

1) Case with Propagation Distance of $10m$*:* As illustrated in Fig. 4a, we can observe the HV indicator values of various algorithms during evolution. The rank of employed MOEAs can be summarized as DPCCMOLSEA $>$ DPCCMOLSIA $>$ CMODE $\approx$ DPCCMOEA $>$ MOEA/D $>$ MOEA/DVA $>$ NSGA-II $\approx$ CCGDE3 $>$ NSGA-III.

As to the convergence speed, DPCCMOLSIA ranks the first, followed is MOEA/D, the third tier includes DPCCMOLSEA, CMODE, DPCCMOEA and CCGDE3, the next is NSGA-II, then NSGA-III, and the last is MOEA/DVA. However, for CCGDE3, there is almost no more improvement and even degradation in the following evolution, while CCGDE3 can obtain similar result to NSGA-II and better performance than NSGA-III. Though DPCCMOLSIA is better than DPCCMOLSEA in the early stage, it is surpassed by DPCCMOLSEA in the following evolution. DPCCMOEA and CMODE are quite similar, while CMODE is a little superior. Owing to the DVA in MOEA/DVA, the HV indicator remains at a low value in the prior stage, though it improve quite fast in the following evolution, finally ranked the sixth, right after MOEA/D.

Fig. 4b illustrates the visualization of the approximated Pareto fronts after 24 runs of each MOEA. For the *Coverage* objective f_{COV}, as illustrated in Fig. 4c and Fig. 4d, MOEA/D, MOEA/DVA, DPCCMOEA, DPCCMOLSEA and DPCCMOLSIA can obtain function values approximately zero, indicating that each wireless device can almost connect to all communicable neighbors within its communication range. Comparatively, CMODE is a little worse, followed are NSGA-II and NSGA-III, and the worst is CCGDE3. When all devices are fully connected, specifically, MOEA/D can guarantee better propagation intensity (*i.e.*, lower f_{PRI} function values), while those of MOEA/DVA, DPCCMOEA, DPCCMOLSEA and DPCCMOLSIA vary little, as detailed in Fig. 4c. While simultaneously considering objectives of *Coverage* and *Interference Intensity* as in Fig. 4d, under the prerequisite of full connection, DPCCMOEA is the best, MOEA/D is comparable, and followed are MOEA/DVA, DPCCMOLSEA and DPCCMOLSIA. In Fig. 4e, we can observe f_{INT} varies approximately from 0.1 to 0.5, much greater than that of f_{PRI}, which has the range of $(0.53, 0.575)$. For the *Propagation Intensity* objective, MOEA/D is the best, while the values of other algorithms not vary much. On the contrary, DPCCMOLSEA and DPCCMOLSIA can achieve much better function values of *Interference Intensity* objective.

2) Case with Propagation Distance of $15m$*:* As illustrated in Fig. 5a, compared to Fig. 4a, the rankings vary little, except that, DPCCMOLSIA is always a little better than DPCCMOLSEA during the whole evolution; CMODE is inferior to DPCCMOEA and MOEA/D, though these three algorithms differ subtly.

We also illustrate the visualization of Pareto fronts when the propagation distance is $15m$ in Fig. 5b to Fig. 5e. With the increment of propagation distance, the neighborhood of each wireless device in enlarged, consequently, the LOS checking and interference constrain are more difficult to satisfy, resulting in severely degraded *Coverage*, as in Fig. 5c and Fig. 5d. In which, we can see that, MOEA/D, MOEA/DVA, DPCC-

TABLE IV: Average Operation Times (secs) of All Algorithms.

TIME	CCGDE3	CMODE	MOEA/D	MOEA/DVA	NSGA-II	NSGA-III	DPCCMOEA	DPCCMOLSEA	DPCCMOLSIA
10m	21506	23466	22885	23570	23357	24025	**338**	**396**	**406**
15m	54631	56126	56745	56275	57636	58533	**825**	**919**	**974**
Speedup	65.47	68.45	68.48	68.66	69.65	71.00	–	**1.13**	**1.19**

[1] Values in bold indicate better results.
[2] The time unit is seconds.

MOEA, DPCCMOLSEA and DPCCMOLSIA can guarantee at least 85% mean average coverage degree. Among which, MOEA/DVA and DPCCMOLSIA are a little better when considering the objective of *Propagation Intensity* (Fig. 5c), while DPCCMOLSEA is better with respect to the objective of *Interference Intensity* (Fig. 5d). Simultaneously considering objectives of *Propagation Intensity* and *Interference Intensity* as in Fig. 5e, the situation is similar to the prior subsection.

D. Operation Time

We list the time consumption as well as the speedups with respect to DPCCMOEA of all employed MOEAs in TABLE IV. We can know the time consumed by distributed parallel algorithms are much less than those of the serial MOEAs. Specifically, the speedups vary from 65.47 to 71.00, quite close to the ideal speedup (i.e., 72).

VIII. Conclusion

WDCN is one of the next generation network technologies for data centers. In this paper, we study the topology optimization problem of the WDCN. On the basis of a heat map of the radio propagation pattern, through image processing, we construct a propagation model. Moreover, the line-of-sight and interference issues are discussed. By considering different aspects of the topology optimization problem, we formulate three objectives, including coverage, propagation intensity and interference intensity, as well as the connectivity constraint. Then, the employed MOEAs are introduced, which are state-of-the-art serial MOEAs as well as three distributed parallel algorithms. And prior knowledge based grouping is integrated to the distributed parallel MOEAs. Finally, the experimental results demonstrate that the distributed parallel MOEAs can tackle the multi-objective topology optimization problem effectively and efficiently in terms of the optimization performance and the time consumption, respectively.

References

[1] L. Cupelli, T. Schütz, P. Jahangiri, M. Fuchs, A. Monti, and D. Müller, "Data center control strategy for participation in demand response programs," *IEEE Transactions on Industrial Informatics*, vol. 14, DOI 10.1109/TII.2018.2806889, no. 11, pp. 5087–5099, Nov. 2018.

[2] N. Kumar, G. S. Aujla, S. Garg, K. Kaur, R. Ranjan, and S. K. Garg, "Renewable energy-based multi-indexed job classification and container management scheme for sustainability of cloud data centers," *IEEE Transactions on Industrial Informatics*, vol. 15, DOI 10.1109/TI-I.2018.2800693, no. 5, pp. 2947–2957, May. 2019.

[3] Q. Fang, J. Wang, Q. Gong, and M. Song, "Thermal-aware energy management of an HPC data center via two-time-scale control," *IEEE Transactions on Industrial Informatics*, vol. 13, DOI 10.1109/TI-I.2017.2698603, no. 5, pp. 2260–2269, Oct. 2017.

[4] B. Dab, I. Fajjari, and N. Aitsaadi, "Online-batch joint routing and channel allocation for hybrid data center networks," *IEEE Transactions on Network and Service Management*, vol. 14, DOI 10.1109/TNS-M.2017.2744801, no. 4, pp. 831–846, Dec. 2017.

[5] B. R. Rofoee, G. Zervas, Y. Yan, M. Anastasopoulos, A. Tzanakaki, S. Peng, R. Nejabati, and D. Simeonidou, "Hardware virtualized flexible network for wireless data-center optical interconnects [invited]," *IEEE/OSA Journal of Optical Communications and Networking*, vol. 7, DOI 10.1364/JOCN.7.00A526, no. 3, pp. A526–A536, Mar. 2015.

[6] R. Khanna, H. Liu, and T. Rangarajan, "Wireless data center management: Sensor network applications and challenges," *IEEE Microwave Magazine*, vol. 15, DOI 10.1109/MMM.2014.2356151, no. 7, pp. S45–S60, Nov. 2014.

[7] K. Ramachandran, R. Kokku, R. Mahindra, and S. Rangarajan, "60 GHz data-center networking: Wireless=> worry less?" *Spectrum*, vol. 1, pp. 1–11, 2008.

[8] Z. Genc, B. L. Dang, J. Wang, and I. Niemegeers, "Home networking at 60 GHz: challenges and research issues," *annals of telecommunications - annales des télécommunications*, vol. 63, DOI 10.1007/s12243-008-0047-0, no. 9, pp. 501–509, Oct. 2008. [Online]. Available: https://doi.org/10.1007/s12243-008-0047-0

[9] J. Guillory, Y. A. Yahia, A. Pizzinat, B. Charbonnier, C. Algani, M. D. Rosales, and J. L. Polleux, "Comparison between two 60GHz multipoint RoF architectures for the home area network," in *2012 17th European Conference on Networks and Optical Communications*, DOI 10.1109/NOC.2012.6249908, pp. 1–5, Jun. 2012.

[10] D. He, J. Portilla, and T. Riesgo, "A 3D multi-objective optimization planning algorithm for wireless sensor networks," in *IECON 2013 - 39th Annual Conference of the IEEE Industrial Electronics Society*, DOI 10.1109/IECON.2013.6700019, pp. 5428–5433, Nov. 2013.

[11] S. Kandula, J. Padhye, and P. Bahl, "Flyways to de-congest data center networks," in *Acm Workshop on Hot Topics in Networks*, pp. 1–6, 2009.

[12] X. Zhou, Z. Zhang, Y. Zhu, Y. Li, S. Kumar, A. Vahdat, B. Y. Zhao, and H. Zheng, "Mirror mirror on the ceiling: Flexible wireless links for data centers," in *Proceedings of the ACM SIGCOMM 2012 Conference on Applications, Technologies, Architectures, and Protocols for Computer Communication*, ser. SIGCOMM '12, pp. 443–454, 2012.

[13] C. Zhang, F. Wu, X. Gao, and G. Chen, "Free talk in the air: A hierarchical topology for 60 GHz wireless data center networks," *IEEE/ACM Transactions on Networking*, vol. 25, DOI 10.1109/T-NET.2017.2755670, no. 6, pp. 3723–3737, Dec. 2017.

[14] J.-Y. Shin, E. G. Sirer, H. Weatherspoon, and D. Kirovski, "On the feasibility of completely wireless datacenters," in *Proceedings of the Eighth ACM/IEEE Symposium on Architectures for Networking and Communications Systems*, ser. ANCS '12, DOI 10.1145/2396556.2396560, pp. 3–14. New York, NY, USA: ACM, 2012. [Online]. Available: http://doi.acm.org/10.1145/2396556.2396560

[15] A. Khonsari, S. P. Shariatpanahi, A. Diyanat, and H. Shafiei, "On the feasibility of wireless interconnects for high-throughput data centers," *Computer Science*, 2015. [Online]. Available: http://arxiv.org/abs/1506.03551v1

[16] K. Deb, A. Pratap, S. Agarwal, and T. Meyarivan, "A fast and elitist multi-objective genetic algorithm: NSGA-II," *IEEE Trans. Evol. Comput.*, vol. 6, no. 2, pp. 182–197, Apr. 2002.

[17] Q. Zhang and H. Li, "MOEA/D: A multiobjective evolutionary algorithm based on decomposition," *IEEE Trans. Evol. Comput.*, vol. 11, no. 6, pp. 712–731, Dec. 2007.

[18] R. C. Gonzalez and R. E. Woods, *Digital Image Processing*, 4th ed. Pearson, 2017.

[19] D. Hearn and M. P. Baker, *Computer Graphics*. Englewood Cliffs, NJ, USA: Prentice Hall, 1994.

[20] L. M. Antonio and C. A. C. Coello, "Use of cooperative coevolution for solving large-scale multi-objective optimization problems," in *2013 IEEE Congr. Evol. Comput.*, pp. 2758–2765, Cancun, Mexico, 2013.

[21] J. Wang, W. Zhang, and J. Zhang, "Cooperative differential evolution with multiple populations for multiobjective optimization," *IEEE Transactions on Cybernetics*, vol. 46, DOI 10.1109/TCYB.2015.2490669, no. 12, pp. 2848–2861, Dec. 2016.

[22] X. Ma and et al., "A multi-objective evolutionary algorithm based on decision variable analyses for multi-objective optimization problems with large-scale variables," *IEEE Trans. Evol. Comput.*, vol. 20, no. 2, pp. 275–298, Apr. 2016.

[23] K. Deb and H. Jain, "An evolutionary many-objective optimization algorithm using reference-point-based nondominated sorting approach, part I: Solving problems with box constraints," *IEEE Transactions on Evolutionary Computation*, vol. 18, DOI 10.1109/TEVC.2013.2281535, no. 4, pp. 577–601, Aug. 2014.

[24] B. Cao, J. Zhao, Z. Lv, and X. Liu, "A distributed parallel cooperative coevolutionary multiobjective evolutionary algorithm for large-scale optimization," *IEEE Transactions on Industrial Informatics*, vol. 13, DOI 10.1109/TII.2017.2676000, no. 4, pp. 2030–2038, Aug. 2017.

[25] B. Cao, J. Zhao, P. Yang, Z. Lv, X. Liu, and G. Min, "3-D multiobjective deployment of an industrial wireless sensor network for maritime applications utilizing a distributed parallel algorithm," *IEEE Transactions on Industrial Informatics*, vol. 14, DOI 10.1109/TII.2018.2803758, no. 12, pp. 5487–5495, Dec. 2018.

[26] B. Cao, J. Zhao, P. Yang, Z. Lv, X. Liu, X. Kang, S. Yang, K. Kang, and A. Anvari-Moghaddam, "Distributed parallel cooperative coevolutionary multi-objective large-scale immune algorithm for deployment of wireless sensor networks," *Future Generation Computer Systems*, vol. 82, DOI https://doi.org/10.1016/j.future.2017.10.015, pp. 256 – 267, 2018. [Online]. Available: http://www.sciencedirect.com/science/article/pii/S0167739X17313523

[27] Y.-J. Gong, W.-N. Chen, Z.-H. Zhan, J. Zhang, Y. Li, Q. Zhang, and J.-J. Li, "Distributed evolutionary algorithms and their models: A survey of the state-of-the-art," *Applied Soft Computing*, vol. 34, DOI https://doi.org/10.1016/j.asoc.2015.04.061, pp. 286 – 300, 2015. [Online]. Available: http://www.sciencedirect.com/science/article/pii/S1568494615002987

[28] R. Storn and K. Price, "Differential evolution – a simple and efficient heuristic for global optimization over continuous spaces," *Journal of Global Optimization*, vol. 11, DOI 10.1023/A:1008202821328, no. 4, pp. 341–359, 1997. [Online]. Available: http://dx.doi.org/10.1023/A:1008202821328

[29] E. Zitzler, L. Thiele, M. Laumanns, C. M. Fonseca, and V. G. da Fonseca, "Performance assessment of multiobjective optimizers: An analysis and review," *IEEE Trans. Evol. Comput.*, vol. 7, no. 2, pp. 117–132, Apr. 2003.